ACS Macro Letters

Letter

pubs.acs.org/macroletters

Solventless High Throughput Manufacturing of Poly(butylene terephthalate) Nanofibers

Kadhiravan Shanmuganathan,[†,§] Yichen Fang,[†,§] Daniel Y. Chou,[†] Sarah Sparks,[†] Jarett Hibbert,[†] and Christopher J. Ellison*[,†,‡]

[†]Department of Chemical Engineering and [‡]Texas Materials Institute, University of Texas Austin, 1 University Station C0400, Austin, Texas 78712, United States

Supporting Information

ABSTRACT: Nanofibers possess high surface area to volume ratios and are particularly attractive for a variety of applications including tissue regeneration, drug delivery, fiber-reinforced composites, filtration, and protective clothing. Though the production of nanofibers from common thermoplastic polymers is relatively well-demonstrated, processing constraints have limited high throughput manufacturing of nanofibers from high performance polymers. This has in turn limited broad technological exploitation of polymer nanofibers in areas such as hot chemical filtration or high-performance lightweight composites for aerospace and defense applications. We report here that nanofibers can be produced in a solventless high throughput process from polymers such as poly(butylene terephthalate) (PBT) using a newly developed technology termed "Forcespinning" that employs centrifugal force to attenuate fibers. Our investigations also show that these nanofibers have a high crystallinity and enhanced molecular orientation which is important for realizing desirable physical and chemical properties of many high-performance polymer fibers.

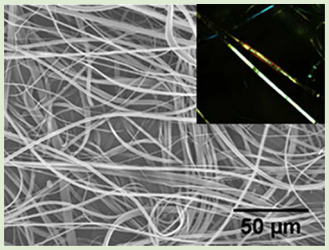

Until recently, electrospinning[1,2] and melt blowing[3] have been the only available techniques for spinning nanofibers. A typical electrospinning process involves application of an electric field to a polymer solution or melt that is delivered at a constant rate through a syringe needle. At a critical applied voltage, electrostatic forces in the fluid overcome surface tension forces, causing a fluid jet emerging from the syringe needle to accelerate toward a grounded collector. As the jet travels toward and deposits on the collector, it undergoes a series of instabilities that are believed to substantially stretch the fluid before it solidifies. Upon evaporation of solvent or cooling of the melt, solid fibers are deposited on the grounded collector.[4] Solution electrospinning has been the more commonly used method to produce nanofibers from common polymers[5−7] or ceramic precursors.[8−10] While melt electrospinning is being developed to overcome solvent recovery challenges and the low productivity of solution electrospinning, the resulting average fiber diameter is typically large,[11−13] with an exception being polymers[14] such as polypropylene where special additives and processing conditions are required to make nanofibers. Melt blowing, which involves extruding a molten polymer through an orifice and stretching the molten polymer using a high pressure hot air jet,[3] is another approach to spin thin fibers. However, this process typically yields fibers of ca. 1−3 μm diameter.

While commercial production of large quantities of nanofibers from commodity polymers is still challenging, it is an even greater challenge to make nanofibers from high performance polymers such as poly(butylene terephthalate) (PBT). These polymers do not dissolve in common organic solvents and typically have high melting temperatures required for demanding applications. PBT, a semicrystalline engineering thermoplastic polymer belonging to the class of linear aromatic polyesters, is well-known for its excellent chemical resistance, thermal stability, mechanical behavior, electrical resistance, low moisture absorption, and so forth.[15] The high rate of crystallization of PBT as compared to poly(ethylene terephthalate) (PET)[16] leads to shorter cycle times in injection molding, and hence this polymer has been used for a variety of applications in automobile parts, electrical components, and consumer goods.[17,18] PBT nanofibers with superior chemical resistance are very attractive for the filtration of physiological fluids and hot chemicals. Moreover, these nanofibers are a candidate to replace PET in tissue engineering applications as scaffolds for endothelial cells.[19] However, PBT suffers from very limited solubility in common organic solvents, and hence electrospinning of PBT nanofibers is typically performed with solvents such as trifluoroacetic acid or hexafluoropropanol.[18,20] Apart from solvent recovery and productivity issues associated with electrospinning, these solvents may not be suitable for certain applications where solvent accumulation or toxicity is a major concern. Recently, Ellison et al.[21] demonstrated that melt blowing could be used to spin PBT nanofibers under special conditions. However, the process requires a very high velocity hot air jet which is energy-intensive. Using a newly developed technology termed "Forcespinning", which overcomes many of these aforementioned challenges, the present study reveals a new pathway for high throughput melt extrusion of PBT

Received: April 23, 2012
Accepted: July 2, 2012
Published: July 13, 2012

   dx.doi.org/10.1021/mz3001995 | *ACS Macro Lett.* 2012, 1, 960−964

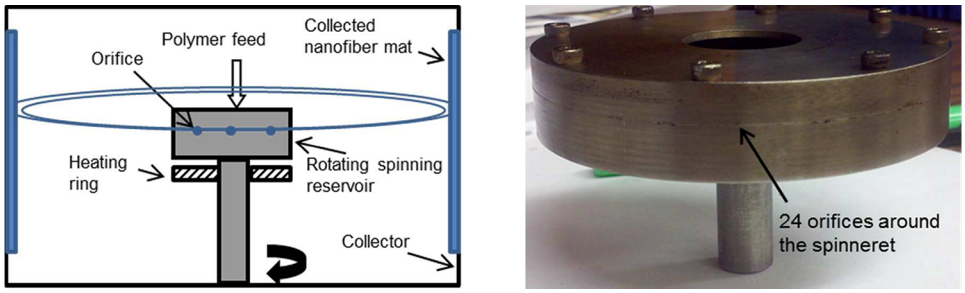

Figure 1. Schematic representation of the Forcespinning process and an image of an actual spinneret used to spin PBT fibers.

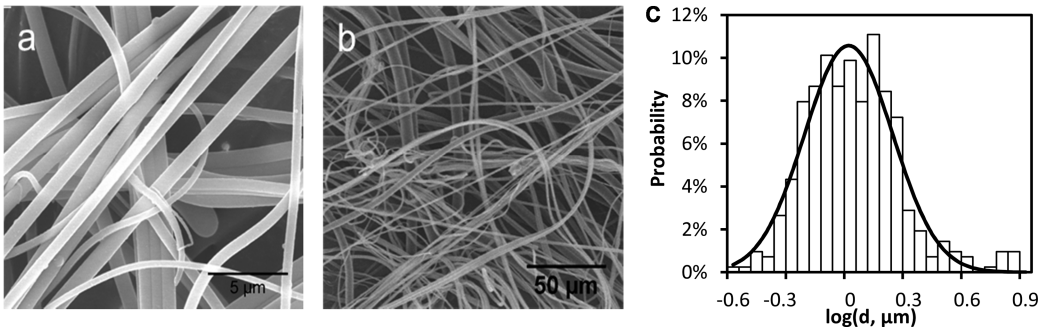

Figure 2. Representative SEM images of PBT nanofibers extruded at 12 000 rpm and 320 °C at (a) high magnification and (b) low magnification. (c) Fiber diameter distribution for the same sample on a logarithmic scale fit to a normal distribution.

Table 1. Average Fiber Diameter and Diameter Distribution Information for PBT Fibers Made by the Forcespinning Process

sample	Rotational speed (rpm)	temperature (°C)	average fiber diameter (μm)	std. dev.	% nanofibers	25th percentile (μm)	50th percentile (μm)	75th percentile (μm)
A	10000	300	1.35	0.78	36.3	0.85	1.20	1.67
B	12000	300	1.31	0.68	40.4	0.79	1.19	1.67
C	15000	300	1.38	0.68	28.0	0.96	1.26	1.61
D	12000	280	1.64	0.90	25.8	0.99	1.53	2.04
E	12000	320	1.17	0.92	54.7	0.66	0.94	1.36

nanofibers with high crystallinity and enhanced molecular orientation. The concept of Forcespinning technology was developed very recently by Lozano et al.[22,23] and employs centrifugal force to attenuate the fibers. In this process, solid polymer or a polymer solution is fed into a spinneret (heated when melt processing) with multiple orifices around its periphery (Figure 1). The rotation of the spinneret at very high speeds (0−20 000 rpm) drives the fluid through the orifices. When the centrifugal force and associated hydrostatic pressure exceeds capillary forces that tend to restrict the flow of fluid in the orifice, a jet of molten polymer is ejected. Centrifugal forces attenuate the fluid jet as it rapidly solidifies into ultrathin fibers at the collector. Though the phenomenon of centrifugal force-based spinning is familiar to anyone that has observed cotton candy being made, there are few reports demonstrating its capabilities as a nanofiber manufacturing technology. For example, Badrossamy et al.[24] used centrifugal force based spinning to show that nanofibers could be made from solutions of common polymers. However, the demonstration of nanofiber production by this process from polymer melts, especially from high performance polymers, is a critical area of research in terms of industrial applications and establishing the process latitude of this new technology.

We report here the first melt extrusion of PBT nanofibers using the Forcespinning process. The percentage of nanofibers (based on the ratio of number of submicrometer diameter fibers to the total number of fibers in the sampling) was as high as 55%, with a range of 300 nm to several micrometers and an average fiber diameter close to 1 μm in most cases. This is especially interesting given the high mass throughput of this melt process compared to solution electrospinning. Figure 2a,b shows scanning electron microscopy (SEM) images of PBT nanofibers made at 12 000 rpm and 320 °C, and Table 1 contains the average diameter and distribution information for this sample and a range of other processing conditions. Additional SEM images of fibers made under different processing conditions can be found in the Supporting Information. As shown in Figure 2b,c for one sample, fiber diameter distributions appear to follow a log-normal function; this sample exhibits an average log(diameter, micrometers) of −0.0076 and a standard deviation of 0.23. Large fibers (>4 μm), such as those in the background of Figure 2b, are very sparse (1 or 2 out of 200 fibers); it could be that they are only generated as the spinneret accelerates to its final speed during startup.

To ensure reproducibility of the results, two batches of fibers were made independently for each condition, and all low and high magnification images were analyzed by separate researchers using image analysis software (Image J, National Institute of Health, US). The average fiber diameter and other data related to fiber dimensions are based on the average of all

dx.doi.org/10.1021/mz3001995 | ACS Macro Lett. 2012, 1, 960−964

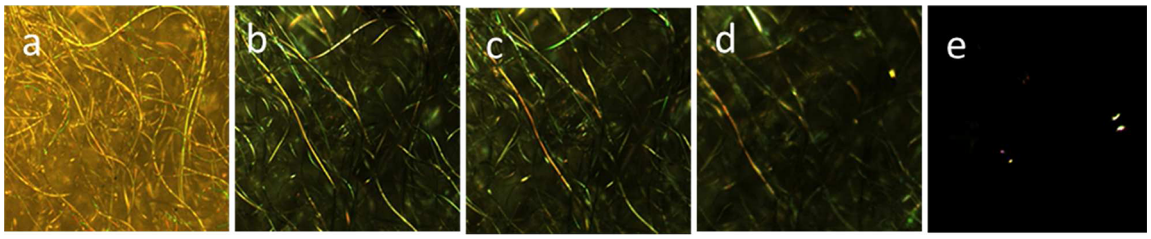

Figure 3. Polarized optical microscopy images at 10× magnification, showing birefringence behavior indicative of a high degree of molecular orientation in PBT fibers. From left to right: (a) without cross polars at room temperature, (b) with cross polars at room temperature, (c) with cross polars at 200 °C, (d) with cross polars at 220 °C, and (e) with cross polars at 240 °C.

measurements that were made (more than a few hundred per sample with random image sampling).

The fiber morphology and diameter are influenced by several variables including spinneret rotational speed (rpm), polymer melt/spinneret temperature, orifice diameter, and collector distance. Our systematic investigations revealed that temperature has a stronger effect on fiber characteristics relative to other factors. Increasing the spinneret temperature from 280 to 320 °C led to a significant increase in percentage of submicrometer fibers from 26 to 55%. The effect of processing temperature can influence fiber formation in different ways. First, increasing the extrusion temperature allows the polymer jet to remain in a molten state for a longer period of time promoting additional stretching before solidification by crystallization. The fiber cools rapidly due to its exposure to ambient air after it is ejected from the spinneret. Second, the temperature has a significant effect on polymer melt viscosity. In fact, dynamic shear experiments revealed nearly an order of magnitude reduction in shear viscosity of PBT from 14.56 Pa·s at 280 °C to 0.88 Pa·s at 320 °C at 1 Hz (see the Supporting Information). So the thinner fibers obtained at higher extrusion temperatures could be due to lower viscosity and/or additional stretching before sufficient cooling takes place for the onset of crystallization. With the fast crystallization kinetics of PBT, it is likely that the difference between the process and crystallization temperature has a more dominant effect than viscosity in controlling the fiber diameter population. This will be the subject of future investigations.

Spinneret rotational speed has a more subtle effect on fiber formation for the conditions evaluated here with PBT. Below a speed of 10 000 rpm, a majority of fibers were between 1 and 3 μm in diameter (data not shown here). Increasing the speed to 10 000 or 12 000 rpm resulted in a significant increase in the nanofiber population. While average fiber diameter was approximately the same, the percentage of submicrometer diameter fibers reduced slightly as the speed was increased from 10 000 or 12 000 to 15 000 rpm. At first glance, this appears counterintuitive as one may expect higher spinneret speeds to produce smaller fibers from enhanced stretching of the fiber with higher centrifugal forces. However, an important feature of this process is that it does not require a positive displacement feed system to deliver the melt through the orifice. In fact, the polymer mass flow rate through the spinneret is partially governed by pressure driven flow from the outward centrifugal force acting on the melt at the spinneret entrance. Thus it appears that it is possible that higher melt flow rates and associated larger fiber populations can result from higher rotational speed under some circumstances.

An attractive aspect of these PBT nanofibers is their high crystallinity and enhanced molecular orientation. Polarized optical microscopy (Figure 3) of PBT fibers revealed birefringence behavior indicative of enhanced molecular orientation from the fiber stretching process. The birefringence diminished as the fibers were taken above 220 °C, near the melting point of the polymer. Irrespective of spinning speed, all PBT nanofibers displayed a high level of crystallinity (~40%), close to or slightly higher than bulk PBT pellets (Table 2). This

Table 2. Melting and Crystallinity Data of the PBT Resin and PBT Nanofibers Made at Various Rotational Speeds at 300 °C[a]

sample	T_m (°C)	T_{crys} (°C)	% crystallinity
PBT pellet	227 ± 1	181 ± 1	39.1 ± 0.8
fibers 10 000 rpm	220 ± 1	196 ± 1	38.4 ± 1.3
fibers 12 000 rpm	221 ± 1	193 ± 1	39.8 ± 0.5
fibers 15 000 rpm	221 ± 1	196 ± 1	42.0 ± 0.4

[a] ± in temperature is standard instrument error, while ± in crystallinity is the standard deviation from three independent measurements.

is significantly different from what is generally observed in electrospun semicrystalline nanofibers, where the crystallinity of as-spun fibers is typically low[25−28] and post processing is required to improve crystallinity. Though one could argue that fast crystallization characteristics of PBT are helping to attain a higher degree of crystallinity, it is important to note that solution electrospun PBT nanofibers have a lower crystallinity than the bulk resin.[18] Although the fibers processed here at different spinning speeds displayed a similar melting behavior, the peak melting temperature of the fibers was 6−7 °C lower than that of the bulk PBT resin (Figure 4 and Table 2). This could be due to smaller crystals or the presence of larger amounts of surface in nanofibers as compared to a bulk polymer. PBT is also known to exhibit polymorphic behavior with an α-crystal phase characterized by gauche−trans−gauche conformation of the four methylene segments and a β-crystal phase characterized by an extended all-trans conformation of the four methylene segments. Studies also report that the α-crystal phase is typically formed under relaxed crystallization conditions while the β-crystal phase is formed under stress.[29] The high extensional stress conditions present in the Forcespinning process and the confined geometry of nanofibers could favor specific crystal morphologies which may result in a shift in the peak melting temperature. We intend to investigate this in detail by X-ray diffraction and report the results in a separate manuscript.

In the subsequent cooling scan (Figure 4b), the PBT resin displayed a very broad crystallization exotherm with a peak at 181 °C, while all PBT fibers exhibited very narrow crystallization exotherms with peak crystallization temperatures between 193 and 196 °C. The molecular orientation present in

dx.doi.org/10.1021/mz3001995 | ACS Macro Lett. 2012, 1, 960−964

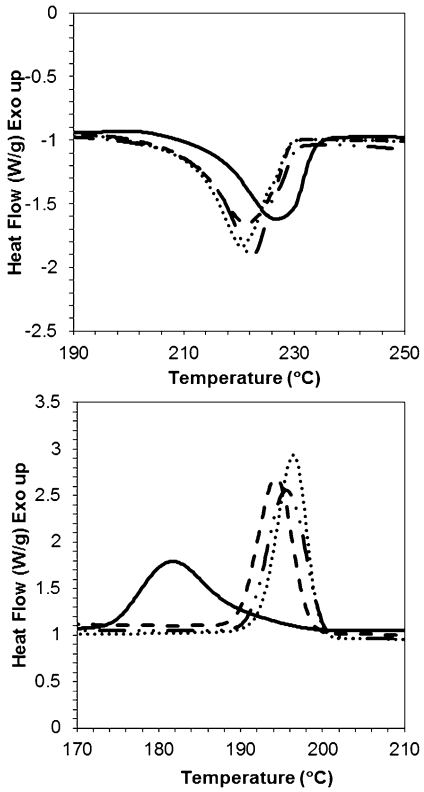

Figure 4. Differential scanning calorimetry thermograms of PBT nanofibers upon first heating (top) and subsequent cooling (bottom), both at 10 °C/min. PBT pellet (solid line), PBT fibers at 10 000 rpm (dotted line), PBT fibers at 12 000 rpm (dashed line), PBT fibers at 15 000 rpm (dash−dot line).

the fibers is probably not completely erased in the first heating scan which could affect later crystallization processes. Completely erasing the memory of the fiber structure could require annealing for long periods of time, longer than were employed in this study. Nonetheless, the intrinsic molecular orientation and confinement effect induced by the fiber structure could enhance the number of nucleation sites, increasing the crystallization temperature. An important finding is that the thermo-mechanical history applied to PBT nanofibers during Forcespinning seems to help to attain enhanced molecular orientation and high crystallinity, two key features that contribute strongly to ultimate mechanical behavior and chemical stability of high-performance semi-crystalline polymer fibers.

This study has demonstrated a facile approach for high throughput manufacturing of nanofibers from a high performance PBT polymer that does not dissolve in common organic solvents and which has high thermal/chemical stability. The fibers are smooth and defect-free with very good chemical resistance. For example, after stirring in hot toluene at 60 °C for 24 h the fibers remain intact with smooth surfaces (Figure 5). While the fiber diameters fall within a range of 300 nm to several micrometers, we have shown that under optimized process conditions the population of submicrometer fibers can be as high as 55% with an average diameter close to 1 μm. Most interestingly, the actual production time for a gram of polymer nanofibers is less than two minutes in this batch process. While this study has revealed some very important capabilities of this process, a more thorough systematic investigation is forthcoming regarding the role of the fluid viscosity, fluid elasticity, and solidification temperature in defining fiber formation.

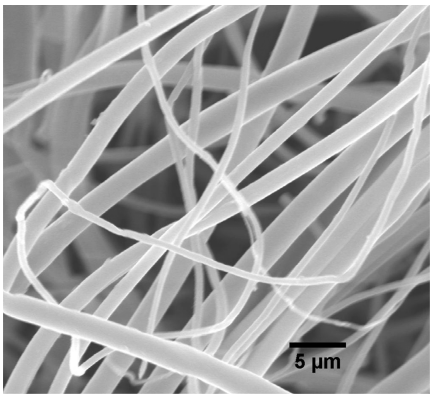

Figure 5. SEM image of fibers made at 12 000 rpm at 300 °C after immersion in hot toluene at 60 °C for 24 h.

EXPERIMENTAL DETAILS

Poly(butylene terephthalate) (PBT) (Celanex 2008) was kindly donated by Ticona USA and used as received. The reported values of melting temperature and density of PBT are 228 °C and 1.38−1.55 g/cm^3.

PBT nanofibers were made by Forcespinning technology using a Cyclone L-1000 M (FibeRio Technology Corp., TX, USA). A 30 gauge stainless steel spinneret (89 mm in diameter) with 24 equally circumferentially spaced orifices (0.25 mm i.d) was used. In this set up, the spinneret assembly is generally heated from the top and bottom with temperature-controlled radiant heater rings. Preheating the spinneret to the desired processing temperature and conducting 2−3 short (30 s) dry run (without polymer) cycles helps to attain a stable temperature rapidly with the polymer being added after the desired temperature is achieved.

PBT fibers were spun at different spin speeds (10 000, 12 000, and 15 000 rpm) and temperatures (280, 300, and 320 °C). For each run, the spinneret was heated to the desired temperature, and then approximately 0.25 g of PBT pellets were added through the spinneret opening in the top. As the pellets melted, the temperature of the polymer melt was monitored with a thermocouple, and when the desired temperature was reached fiber spinning was started. This ensured that the pellets were heated quickly (within 4−5 min) to minimize sample degradation from oxygen and heat exposure. Molten PBT was driven through the spinneret orifices due to centrifugal force during spinning. Cooled and solidified fibers were collected on the circular plate collector located 15 cm away from the spinneret. After each experiment, a purge run was conducted to clear any residual polymer from the spinneret.

ASSOCIATED CONTENT

Supporting Information

Additional experimental details, SEM images, and rheology data. This material is available free of charge via the Internet at http://pubs.acs.org.

AUTHOR INFORMATION

Corresponding Author

*E-mail: ellison@che.utexas.edu.

Author Contributions

§These authors contributed equally.

Notes

The authors declare no competing financial interest.

■ ACKNOWLEDGMENTS

The authors thank C. Grant Willson for permitting the use of his SEM facility.

■ REFERENCES

(1) Shin, Y. M.; Hohman, M. M.; Brenner, M. P.; Rutledge, G. C. *Appl. Phys. Lett.* **2001**, *78*, 1149.
(2) Doshi, J.; Reneker, D. H. *J. Electrost.* **1995**, *35*, 151.
(3) Tan, D. H.; Zhou, C. F.; Ellison, C. J.; Kumar, S.; Macosko, C. W.; Bates, F. S. *J. Non-Newtonian Fluid Mech.* **2010**, *165*, 892.
(4) Reneker, D. H.; Yarin, A. L.; Fong, H.; Koombhongse, S. *J. Appl. Phys.* **2000**, *87*, 4531.
(5) Dong, B.; Arnoult, O.; Smith, M. E.; Wnek, G. E. *Macromol. Rapid Commun.* **2009**, *30*, 539.
(6) Prabhakaran, M. P.; Venugopal, J.; Ramakrishna, S. *Acta Biomater.* **2009**, *5*, 2884.
(7) Choi, J.; Lee, K. M.; Wycisk, R.; Pintauro, P. N.; Mather, P. T. *Macromolecules* **2008**, *41*, 4569.
(8) Li, Z.; Zhang, H.; Zheng, W.; Wang, W.; Huang, H.; Wang, C.; MacDiarmid, A. G.; Wei, Y. *J. Am. Chem. Soc.* **2008**, *130*, 5036.
(9) Kumar, A.; Jose, R.; Fujihara, K.; Wang, J.; Ramakrishna, S. *Chem. Mater.* **2007**, *19*, 6536.
(10) Formo, E.; Lee, E.; Campbell, D.; Xia, Y. *Nano Lett.* **2008**, *8*, 668.
(11) Lyons, J.; Li, C.; Ko, F. *Polymer* **2004**, *45*, 7597.
(12) Dalton, P. D.; Klinkhammer, K.; Salber, J.; Klee, D.; Möller, M. *Biomacromolecules* **2006**, *7*, 686.
(13) Agarwal, S.; Greiner, A.; Wendorff, J. H. *Adv. Funct. Mater.* **2009**, *19*, 2863.
(14) Dalton, P. D.; Grafahrend, D.; Klinkhammer, K.; Klee, D.; Moller, M. *Polymer* **2007**, *48*, 6823.
(15) Deshmukh, G. S.; Peshwe, D. R.; Pathak, S. U.; Ekhe, J. D. *J. Polym. Res.* **2011**, *18*, 1081.
(16) Chuah, H. H. *Polym. Eng. Sci.* **2001**, *41*, 308.
(17) Banik, K.; Mennig, G. *Polym. Eng. Sci.* **2008**, *48*, 957.
(18) Catalani, L. H.; Collins, G.; Jaffe, M. *Macromolecules* **2007**, *40*, 1693.
(19) Ma, Z.; Kotaki, M.; Yong, T.; He, W.; Ramakrishna, S. *Biomaterials* **2005**, *26*, 2527.
(20) Forouharshad, M.; Saligheh, O.; Arasteh, R.; Farsani, R. E. *J. Macromol. Sci., Part B: Phys.* **2010**, *49*, 833.
(21) Ellison, C. J.; Phatak, A.; Giles, D. W.; Macosko, C. W.; Bates, F. S. *Polymer* **2007**, *48*, 3306.
(22) Sarkar, K.; Gomez, C.; Zambrano, S.; Ramirez, M.; de Hoyos, E.; Vasquez, H.; Lozano, K. *Mater. Today* **2010**, *13*, 12.
(23) Padron, S.; Patlan, R.; Gutierrez, J.; Santos, N.; Eubanks, T.; Lozano, K. *J. Appl. Polym. Sci.* **2012**, DOI: 10.1002/app.36420.
(24) Badrossamay, M. R.; McIlwee, H. A.; Goss, J. A.; Parker, K. K. *Nano Lett.* **2010**, *10*, 2257.
(25) Zong, X.; Kim, K.; Fang, D.; Ran, S.; Hsiao, B. S.; Chu, B. *Polymer* **2002**, *43*, 4403.
(26) Zhou, H. J.; Green, T. B.; Joo, Y. L. *Polymer* **2006**, *47*, 7497.
(27) Wang, M.; Jin, H.-J.; Kaplan, D. L.; Rutledge, G. C. *Macromolecules* **2004**, *37*, 6856.
(28) Wang, D.; Sun, G.; Chiou, B.-S.; Hinestroza, J. P. *Polym. Eng. Sci.* **2007**, *47*, 1865.
(29) Carr, P. L.; Jakeways, R.; Klein, J. L.; Ward, I. M. *J. Polym. Sci., Part B: Polym. Phys.* **1997**, *35*, 2465.